FULL PAPER

Synthesis and Structural Characterization of Multi-Molybdenum substituted Preyssler-type Phosphotungstates

Muh. Nur Khoiru Wihadi,[a,b] Terufumi Haioka,[a] Tatsuhiro Kojima,[c] Xavier López,[d] Tadaharu Ueda,[e,f] Tsuneji Sano,[a] and Masahiro Sadakane*[a]

Dedication ((optional))

Abstract: We report synthesis of multi-Mo-substituted Preyssler-type phosphotungstates, $[P_5W_{30-x}Mo_xO_{110}Na(H_2O)]^{14-}$, with different amount of incorporated Mo via hydrothermal reactions of H_3PO_4, Na_2WO_4, and Na_2MoO_4, and characterization by ^{31}P NMR, FT-IR, elemental analysis, ESI-MS, and cyclic voltammetry. The number of substituted Mo increased by the increasing amount of Na_2MoO_4 in the reaction mixture, and multi-Mo-substituted $[P_5W_{30-x}Mo_xO_{110}Na(H_2O)]^{14-}$, up to Mo of 5 can be produced. Single crystal X-ray structure analysis and density functional theory calculation indicates that the most suitable substitution position is the belt position.

Introduction

Polyoxometalates (POMs) are an interesting family of anionic metal-oxide molecules constructed mainly by early transition metals such as W, Mo, V, and Nb in high oxidation states. The POM family exhibits properties such as multi-electron redox activity, acidic property, photochemistry and magnetism, and has been applied in many fields of functional materials such as catalysis, conducting materials, and magnetic materials.[1,2] Among the wide class of POMs, Preyssler-type phosphotungstates have been attracting much attention, and they have been applied as catalysts,[3–12] single molecule electret materials,[13] single molecule magnetic materials,[14] conductive materials,[15–23] staining reagents,[24] liposome collapse reagents,[25,26] and antibacterial agents.[27–30] Preyssler-type phosphotungstates, $[P_5W_{30}O_{110}Z^{n+}(H_2O)]^{(15-n)-}$, are constructed by five PO_4 tetrahedra surrounded by thirty WO_6 octahedra which created a doughnut-shape structure with an internal cavity space that can encapsulate a cation (Z^{n+}) in the molecule (Figure 1). Cations such as Na^+,[31,32] lanthanide,[4,13,33–36] actinide cations,[33–35,37-38] Ca^{2+},[4,33,37,39] Y^{3+},[4,33,37] Bi^{3+},[4,19,21,33,39] Ag^+,[28–30,40–42] or K^+,[5,6,43–45] can be encapsulated, and replacement of the encapsulated cation is widely used to tune the properties of the Preyssler compound.

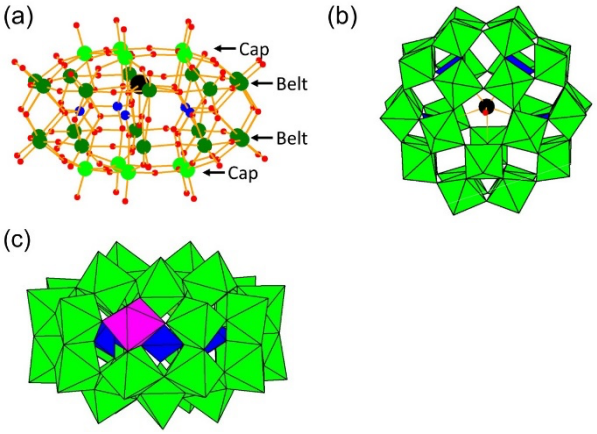

Figure 1. (a) Ball-and-stick and (b) Polyhedral representation of the Preyssler-type phosphotungstate, $[P_5W_{30}O_{110}Na(H_2O)]^{14-}$, with one encapsulated Na and water oxygen. (c) Polyhedral representation of mono-Mo substituted Preyssler-type phosphotungstate where one Mo occupies belt position. Light green, dark green, red, and black balls represent, tungstens on cap position, tungstens on belt position, oxygen, and encapsulated Na, respectively. Green octahedra, blue tetrahedra, and purple octahedron represent, W-O_6 octahedra, P-O_4 tetrahedra, and Mo-O_6 octahedra, respectively.

An alternative method to tune the properties is substitution of framework W atoms. Pope's group has reported mono-V-substituted species, $[P_5W_{29}VO_{110}Na]^{15-}$, which was prepared by a reaction of $VOSO_4$ with a lacunary Preyssler produced by reacting $[P_5W_{30}O_{110}Na]^{14-}$ with NaOH.[31] Amini's group has reported mono-Mo substituted derivative, $[P_5W_{29}MoO_{110}Na]^{14-}$, by a hydrothermal reaction of H_3PO_4, Na_2WO_4, and Na_2MoO_4 in water.[46] Several research groups of Bamoharram,[7] Amini,[46] Ruiz[47] and

[a] M. N. K. Wihadi, T. Haioka, T. Sano and M. Sadakane*
Department of Applied Chemistry
Graduate School of Advanced Science and Engineering, Hiroshima University
1-4-1 Kagamiyama, Higashi-Hiroshima 739-8527, Japan. Fax: +81 82 424 5494; Tel: +81 82 424 4456
E-mail: sadakane09@hiroshima-u.ac.jp
Homepage URL: home.hiroshima-u.ac.jp/catalche
[b] M. N. K. Wihadi
Research Center for Chemisty
National Research and Innovation Agency Republic of Indonesia
Kawasan Puspiptek, Serpong, Tangerang Selatan 15311, Indonesia
[c] T. Kojima
Department of Chemistry
Graduate School of Science, Osaka University
1-1, Machikaneyama, Toyanaka, Osaka, 560-0043, Japan
[d] X. López
Departament de Química Física i Inorgànica
Universitat Rovira i Virgili
c/Marcel·lí Domingo 1, 43007 Tarragona, Spain
[e] T. Ueda
Department of Marine Resource Science
Faculty of Agriculture and Marine Science, Kochi University
Nankoku, 780-8520, Japan
[f] T. Ueda
Center for Advanced Marine Core Research, Kochi University
Nankoku, 783-8502, Japan

Supporting information for this article is given via a link at the end of the document.

Vázquez[48] have reported improved catalytic activities of $[P_5W_{29}MoO_{110}Na(H_2O)]^{14-}$ for esterification reaction and oxidation reactions. Recently, Schimpf's group has reported that iron-salt of $[P_5W_{29}MoO_{110}Na]^{14-}$ shows higher conductivities than the non-substituted $[P_5W_{30}O_{110}Na]^{14-}$ derivative.[22] They have reported single crystal structure analysis of the potassium salt of $[P_5W_{29}MoO_{110}Na]^{14-}$, and the Mo substituted occurs on the belt position. Therefore, the design of Mo-substituted Preyssler derivatives is important. To the best of our knowledge, no information about multi-Mo substituted derivatives has been reported.

Herein, we report preparation and characterization of multi-Mo substituted Preyssler-type phosphotungstates, $[P_5W_{30-x}Mo_xO_{110}Na(H_2O)]^{14-}$ by a hydrothermal reaction of designated concentrations of H_3PO_4, Na_2WO_4, and Na_2MoO_4.

Results and Discussion

Reaction Condition and Isolation

Hydrothermal reaction of sodium tungstate (Na_2WO_4) and phosphoric acid (H_3PO_4) with different amount (W:Mo = 30:0, 27:3, 25:5, 22:8, 20:10, 17:13, 9:21, 3:27 or 0:30) of sodium molybdate (Na_2MoO_4) were performed (Table 1). After the reaction mixture was cooled down to room temperature, precipitates were obtained when the Mo amount was lower than W:Mo = 20:10 (Table 1, No. 1-5). ^{31}P NMR of the reaction solutions (Figure S1) indicated that signal of $[P_5W_{30}O_{110}Na(H_2O)]^{14-}$ around at -9.62 ppm was observed when the Mo amount was lower than W:Mo = 20:10. The presence of Dawson type $[P_2W_{18}O_{62}]^{6-}$ and its substituted species $[P_2W_{18-x}Mo_xO_{62}]^{6-}$ were also detected at range -11.55 ppm to -12.65 except for samples with W:Mo ratio of 3:27 and 0:30. Characterization of the formed precipitates by IR and ^{31}P NMR indicates these solids were Dawson type species $[P_2W_{18-x}Mo_xO_{62}]^{6-}$ (Figure S2 and S3)[58].

The common procedure to isolate and purify the Preyssler-type phosphotungstate is precipitation by KCl addition to the reaction mixture and subsequent recrystallization of the precipitates. ^{31}P NMR of precipitates after addition of KCl showed signal for $[P_5W_{30}O_{110}Na(H_2O)]^{14-}$ at -9.34 ppm and probably its substituted species $[P_5W_{30-x}Mo_xO_{110}Na(H_2O)]^{14-}$ at -8.47 ppm and -9.49 ppm (Figure S4). The signals correspond to Dawson-type $[P_2W_{18}O_{62}]^{6-}$ was also detected at -12.33 ppm and its substituted species -11.27 ppm and -12.29 ppm correspond to [1-$P_2W_{17}MoO_{62}]^{6-}$ and -11.33 ppm and -12.23 ppm correspond to [4-$P_2W_{17}MoO_{62}]^{6-}$. The phosphate derivatives between -2 and 2 ppm were also presence in the precipitates as impurity. No Preyssler-type phosphotungstate species were detected in the case of low amount of W (Figure S4, samples with W:Mo = 0:30, 3:27 and 9:21).

In order to increase purify of the Preyssler derivatives, we performed recrystallization with an assumption that substitution of W^{6+} with Mo^{6+} did not affect the crystallization behavior of the Preyssler species. After the first recrystallization, phosphate contamination in the solid decreased and Dawson anion derivative was partially separated in the filtrate solution shown in ^{31}P NMR spectroscopy (Figure S5 and S6). However, in this step the Dawson anion and phosphate contamination still existed in the solid. Therefore, we performed the second recrystallization to enhance the purity of Preyssler-type substituted molybdenum (W:Mo = 30:0, 27:3, 25:5, 22:8, 20:10).

Table 1. Ratio of W and Mo in hydrothermal reaction for Preyssler-type compounds, recrystallization condition, and yield

	Reaction mixture[a]		After the reaction		Isolated product
No.	Na_2WO_4 [g] ([mmol])	Na_2MoO_4 [g] ([mmol])	Preyssler in solution[b]	Solid[c]	W:Mo ratio[d]
1.	32.32 (98.0)	0 (0)	Y	Y	
	W:Mo = 30:0				
2.	29.380 (89.1)	2.060 (8.5)	Y	Y	
	W:Mo = 27:3				W:Mo = 28.9:1.1
3.	26.440 (80.0)	4.120 (16.9)	Y	Y	
	W:Mo = 25:5				W:Mo = 27.9:2.1
4.	23.510 (71.2)	6.180 (25.6)	Y	Y	
	W:Mo = 22:8				W:Mo = 27.6:2.4
5.	20.570 (62.5)	8.240 (33.9)	Y	Y	
	W:Mo = 20:10				W:Mo = 26.4:3.6
6.	17.630 (53.4)	10.300 (42.5)	N	N	
	W:Mo = 17:13				
7.	8.820 (26.7)	16.470 (68.0)	N	N	
	9:21				
8.	2.940 (8.9)	20.590 (85.0)	N	N	
	W:Mo = 3:27				
9.	0 (0)	22.650 (93.5)	N	N	
	W:Mo = 0:30				

[a] Na_2WO_4-$2H_2O$, Na_2MoO_4-$2H_2O$, and H_3PO_4 (85%, 26.5 mL) were mixed with water (30 mL) in a Teflon-liner autoclave, and heated at 125 ºC for 24 hours. [b]Y indicates that Preyssler compounds are detected by ^{31}P NMR of the reaction solution after the hydrothermal reaction. [c]Y indicates that solid was obtained after cooling the reaction mixture to room temperature. [d]W:Mo ratio of the solid obtained after the 2nd recrystallization is estimated by ICP.

After the second recrystallization, we obtained the solid without phosphate species and Dawson-type species when W:Mo ratio was 30:0, 27:3, 25:5, 22:8, and 20:10 (Figure 2). All undesired compounds were remained in the filtrate solutions (Figure S7). ^{31}P NMR spectra of the crystals revealed signals at -9.34 ppm assigned to $[P_5W_{30}O_{110}Na(H_2O)]^{14-}$ and several small signals detected at -8.47 ppm, -9.49 ppm and -9.70 ppm.

Structural Characterisation by IR, Elemental Analysis, HR-ESI-MS, DFT calculation and Cyclic Voltammetry

The IR spectra of the solids shows characteristic bands for Preyssler-type phosphotungstate, $[P_5W_{30-x}Mo_xO_{110}Na(H_2O)]^{14-}$ (Figure 3).

The elemental analyses revealed the formula $K_{12.5}Na_{1.5}[P_5W_{28.6}Mo_{1.4}O_{110}Na(H_2O)]$, $K_{12}Na_2[P_5W_{27.9}Mo_{2.1}O_{110}Na(H_2O)]$, $K_{12.5}Na_{1.5}[P_5W_{27.4}Mo_{2.6}O_{110}Na(H_2O)]$ and $K_{12.5}Na_{1.5}[P_5W_{26.5}Mo_{3.5}O_{110}Na(H_2O)]$ for the solids prepared by

different Na_2WO_4:Na_2MoO_4 ratio of 27:3, 25:5, 22:8, and 20:10, respectively. Increasing of the Na_2MoO_4 in the reaction mixture increased amount of Mo in the Preyssler species.

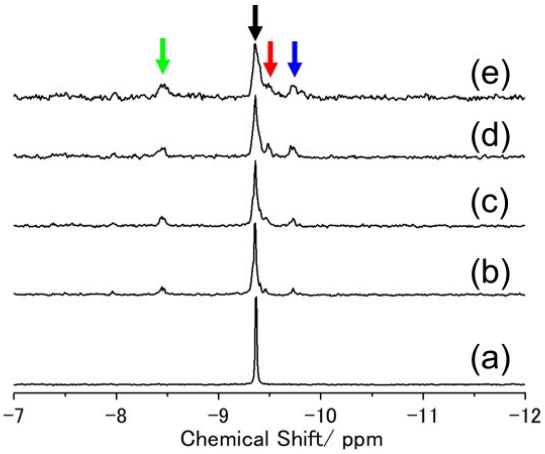

Figure 2. ^{31}P NMR Spectra of solid obtained after 2nd recrystallization with different Na_2WO_4:Na_2MoO_4 ratio of (a) 30:0, (b) 27:3, (c) 25:5, (d) 22:8, and (e) 20:10 in the reaction mixture. The black arrow (δ = -9.34 ppm) correspond to $[P_5W_{30}O_{110}Na(H_2O)]^{14-}$. The red (δ = -9.49 ppm), the blue (δ = -9.70 ppm), and the green (δ = -8.47 ppm) arrows correspond to $[P_5W_{30-x}Mo_xO_{110}Na(H_2O)]^{14-}$ with different number of Mo substitutions.

The isolated solids were analyzed by high resolution electron spray ionization mass spectroscopy (HR-ESI-MS) after dissolved in H_2O-CH_3OH. In the case of non-substituted Preyssler-type phosphotungatate, $[P_5W_{30}O_{110}Na(H_2O)]^{14-}$, profiles which could be assigned to be a mixture of several Preyssler-type phosphotungstates were observed. The four most intense profiles are assignable to $[H_8P_5W_{30}O_{110}K(H_2O)]^{6-}$, $[H_7KP_5W_{30}O_{110}Na(H_2O)]^{6-}$, $[H_7KP_5W_{30}O_{110}K(H_2O)]^{6-}$, and $[H_6K_2P_5W_{30}O_{110}Na(H_2O)]^{6-}$ (Figure S8(a), S9(a), and S10(a)). The mono-Na containing ions such as $[H_7KP_5W_{30}O_{110}Na(H_2O)]^{6-}$ and $[H_6K_2P_5W_{30}O_{110}Na(H_2O)]^{6-}$ were proton-and-potassium mixed salts of the $[P_5W_{30}O_{110}Na(H_2O)]^{14-}$. On the other hand, non-Na containing ions such as $[H_8P_5W_{30}O_{110}K(H_2O)]^{6-}$ and $[H_7KP_5W_{30}O_{110}K(H_2O)]^{6-}$ were potassium encapsulated Preyssler compounds produced under ESI-MS condition. The potassium encapsulated Preyssler-compound, $[P_5W_{30}O_{110}K(H_2O)]^{14-}$, has been reported by Sun's group.[44] We have reported that heating of the potassium salt of sodium-encapsulated anion, $K_{14}[P_5W_{30}O_{110}Na(H_2O)]$, produced mono-potassium and di-potassium encapsulated anion such as $[P_5W_{30}O_{110}K]^{14-}$ and $[P_5W_{30}O_{110}K_2]^{14-}$.[45]

In the case of Mo substituted Preyssler-type phosphotungstates, $[P_5W_{30-x}Mo_xO_{110}Na(H_2O)]^{14-}$, several profiles assignable to Mo-substituted species were observed (Figure S8, S9, and S10). ESI-MS of $[P_5W_{28.9}Mo_{2.1}O_{110}Na(H_2O)]^{14-}$ shows profiles assignable to mono-Mo, di-Mo, and tri-Mo substituted species (Figure 4). Further Mo-substituted species shows profiles assignable to more Mo-substituted species, and penta-Mo-substituted complex was clearly detected in the case of $[P_5W_{26.5}Mo_{3.5}O_{110}Na(H_2O)]^{14-}$.

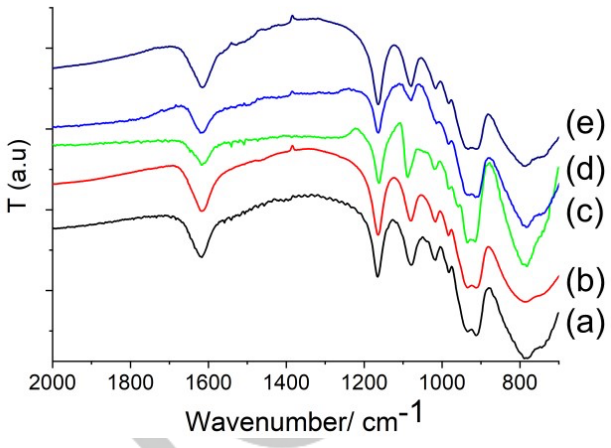

Figure 3 IR Spectra of solid obtained after 2nd recrystallization with different Na_2WO_4:Na_2MoO_4 ratio of (a) 30:0, (b) 27:3, (c) 25:5, (d) 22:8, and (e) 20:10 in the reaction mixture.

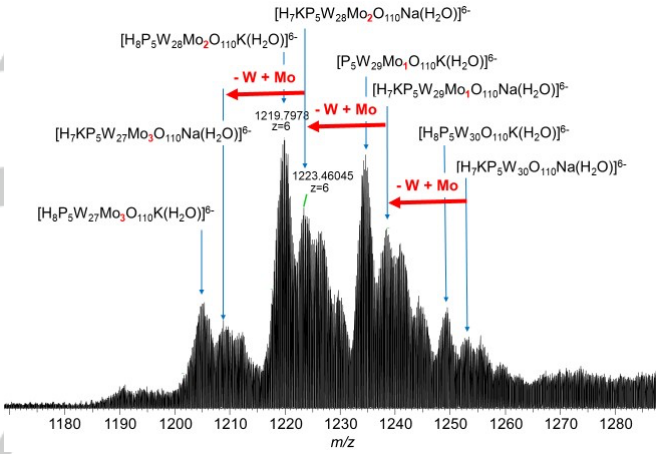

Figure 4. ESI-MS spectrum of $K_{12.5}Na_{1.5}[P_5W_{27.4}Mo_{2.6}O_{110}Na(H_2O)]$ dissolved in H_2O/CH_3OH.

We conclude that we could isolate mixtures of Mo-substituted Preyssler-type phosphotungstates, $[P_5W_{30-x}Mo_xO_{110}Na(H_2O)]^{14-}$ (x up to 5), by the following reasons. 1) Elemental analysis results are consisted to the potassium-sodium mixed salt of the Preyssler-type compounds. 2) ESI-MS spectra showed profiles assignable to the Mo-substituted Preyssler-type phosphotungstates (Figure 4, S8, S9, S10). 3) Although ESI-MS profile indicated that they are mixture with different Mo amount, formula of the most abundant Mo-substituted species by ESI-MS is almost same to the one estimated by elemental analysis (Figure S9). 4) IR spectra showed characteristic bands pattern for the Preyssler-type phosphotungstates (Figure 3). It is known that $H_3PW_{12}O_{40}$ and $H_3PMo_{12}O_{40}$ showed similar pattern with different band positions.[59] In the present case, amount of maximum Mo substituted in the Preyssler framework was 5 according to ESI-MS profiles, and in such low Mo contents IR spectra of the Mo-

substituted Preyssler compounds might be similar to one of non-substituted $[P_5W_{30}O_{110}Na(H_2O)]^{14-}$.

^{31}P NMR signal at -9.34 ppm assignable to non-substituted $[P_5W_{30}O_{110}Na(H_2O)]^{14-}$ became broader and new peaks at -8.47, -9.47, and -9.70 ppm appeared by introduction of Mo. The peak at -9.34 became more broader and the intensities of the new peaks increased by increasing the Mo amount, indicating that these signals are assignable to Mo-substituted species. However, it is now not possible for us to assign all signals.

Five phosphorous in non-substituted complex is equivalent, and therefore only one ^{31}P NMR singlet is observed. ^{183}W NMR of the non-substituted complex shows four singlets, because there are four kinds of W, cap W close to the encapsulated Na, cap W far from the encapsulated Na, belt W close to the encapsulated Na, and belt W far from the encapsulated Na.[4] Mono-Mo substitution of W produces four isomers, and there are three non-equivalent P in each four isomers. Multi-Mo substitution produces more isomers, and more non-equivalent P which makes assignment of ^{31}P NMR difficult.

Schimpf's group has reported single crystal structure analysis of potassium salt of $[P_5W_{29}MoO_{110}Na]^{14-}$ where the Mo substituted occurs on the belt position.[22] We performed single crystal X-ray structure analysis of $K_{12.5}Na_{1.5}[P_5W_{26.5}Mo_{3.5}O_{110}Na(H_2O)]$. Similar to single crystal X-ray structure analysis results of other Preyssler-compounds, $[P_5W_{26.5}Mo_{3.5}O_{110}Na(H_2O)]^{14-}$ crystalized in an *orthorhombic* unit cell with *Pnna* (52) space group and an asymmetric unit contains half of the Preyssler molecule where cap and belt W close to Na are not distinguishable from those far from Na due to disorder of molecule (Figure S11). Our attempt to estimate positions of Mo revealed that W atoms, W_6-W_{15}, on the belt positions are subject to be substituted with Mo atoms rather than those, W_1-W_5, on the cap positions judging from site occupancies of W and Mo atoms, though they are disordered over the belt positions (Table S1).

We performed a DFT study on the four isomers of the mono-Mo substituted compound (Table 2). The belt positions are the most stable for W-Mo substitution. The belt substitution close to the encapsulated Na^+ (Entry 3) revealed higher stability than that far from the Na^+ but only by 0.74 kcal mol^{-1} (Entry 4). The two cap substitutions calculated present higher relative energies of 2.88 and 3.68 kcal mol^{-1} above the lowest energy form (Entries 1 and 2). These values evidence a clear preference of the Mo for belt positions.

Table 2. DFT calculation results for mono-molybdenum substituted Preyssler-type Phosphotungstate, $[P_5W_{29}MoO_{110}Na]^{14-}$

Entry	Substitution Sites Model	Energy (kcal mol^{-1})	Relative energy (kcal mol^{-1})
1	Cap close to Na^+	-29892.51	2.9
2	Cap far from Na^+	-29891.71	3.7
3	Belt close to Na^+	-29895.39	0
4	Belt far from Na^+	-29894.65	0.74

Figure 5 shows the cyclic voltammogram (CV) of the $[P_5W_{30-x}Mo_xO_{110}Na(H_2O)]^{14-}$ series in 0.1 M HCl. The $[P_5W_{30}O_{110}Na(H_2O)]^{14-}$ exhibits two four-electron transfer processes and two-electron transfered one in 1.0 M HCl[33,60], which appeared ad -180 mV and -300 mV and -520 mV, respectively, in 0.1 M HCl. In CVs of $[P_5W_{30-x}Mo_xO_{110}Na(H_2O)]^{14-}$ (Mo:W ratio = 3:27, 5:25, 8:22, and 10:20) new irreversible waves appeared at the region -50 mV to +600 mV with current magniture of waves increased depending on substituted Mo amount which is similar to voltammetric behavior of Keggin-type $[PW_{12-x}Mo_xO_{40}]^{3-}$ (x = 1-11) formed in a 50 mM (W(VI)-Mo(VI)) – 10 mM P(V) – 0.5 M HCl – 50%(v/v) CH_3CN system.[61] These new waves are corresponded to the redox of Mo(VI/V) in molybdenum components of $[P_5W_{30-x}Mo_xO_{110}Na(H_2O)]^{14-}$, because the reduction potentials of molybdenum components are more positive than those of tungsten components in POMs. In addition, irreversible and broad-shaped waves should be ascribed that each of several molybdenums in several isomers of $[P_5W_{30-x}Mo_xO_{110}Na(H_2O)]^{14-}$ generated from incorporation of molybdenum at different positions of framework of Preyssler-type POMs, should be reduced at different potentials.

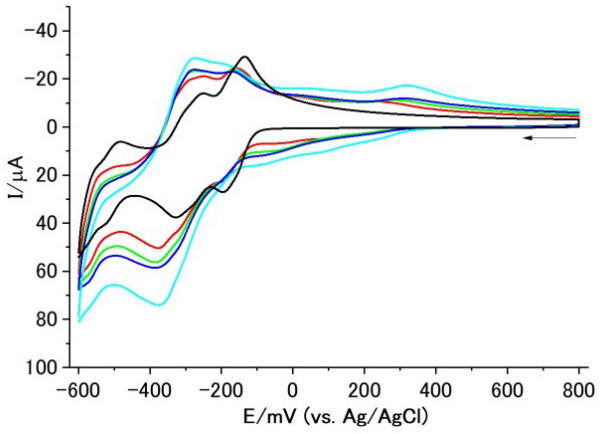

Figure 5. Cyclic Voltammograms of 0.5 mM (black) $K_{14}[P_5W_{30}O_{110}Na(H_2O)]$ (red) $K_{12.5}Na_{1.5}[P_5W_{28.6}Mo_{1.4}O_{110}Na(H_2O)]$, (green) $K_{12}Na_2[P_5W_{27.9}Mo_{2.1}O_{110}Na(H_2O)]$, (blue) $K_{12.5}Na_{1.5}[P_5W_{27.4}Mo_{2.6}O_{110}Na(H_2O)]$ and (cyan) $K_{12.5}Na_{1.5}[P_5W_{26.5}Mo_{3.5}O_{110}Na(H_2O)]$ with different Mo:W ratio from assembly reaction of tungstate and molybdate in 0.1 M HCl. Scan rate was 100 mVs^{-1}.

Conclusions

The first multi-Mo substituted Preyssler-type phosphotungstates, $[P_5W_{30-x}Mo_xO_{110}Na(H_2O)]^{14-}$ has been successfully prepared via self-assembly reaction of sodium tungstate and phosphoric acid in the presence of sodium molybdate under hydrothermal condition. The formation of $[P_5W_{30-x}Mo_xO_{110}Na(H_2O)]^{14-}$ and the number of Mo in the framework was dependent on the W:Mo ratio in the reaction medium. The Preyssler-type substituted framework formed when the reaction conditions were in the range 0 ≤ W:Mo ≤ 20:10. The formation of Dawson-type substituted frameworks

was also found in the products when the reaction conditions were in the range 0 ≤ W:Mo ≤ 9:21. Characterization by IR, ^{31}P NMR, elemental analysis, and ESI-MS confirmed that the isolated solids were a mixture of isomers of different number of incorporated Mo, being possible up to 5 molybdate atoms into the framework to form $[P_5W_{25}Mo_5O_{110}Na(H_2O)]^{14-}$.

Experimental Section

Materials. Homemade deionized water (Millipore, Elix) was used. All chemicals were reagent-grade and used as provided.

Preparation of $K_{14}[P_5W_{30}O_{110}Na(H_2O)]-23H_2O$ (W:Mo = 30:0) $K_{14}[P_5W_{30}O_{110}Na(H_2O)]-23H_2O$ were prepared according to the published procedure[3,4,28]. Na_2WO_4-2H_2O (32.320 g, 98.0 mmol) was mixed with water (30 mL) in a Teflon-lined autoclave reactor, and phosphoric acid (85%, 26.5 mL) was added to the mixture. The reactor was placed in an oven heated at 125 °C for 24 h, and then the reactor was cooled down to room temperature. The yellowish green crystal was obtained which was filtered from the reaction mixture. The water (20 mL) was added to the filtrate followed by addition KCl (10.0 g), and the mixture was stirred for 10 min. The formed precipitates were filtered off, and the solid was dried at 70 °C overnight (ca. 19.086 g). The solid were recrystallized from hot water (95 ºC, 40 mL) using a metal bath and obtained the white crystal which were collected by filtration (yield ca. 9.104 g). The solid were recrystallized again from 13 mL of hot water (95 ºC) and the pure white crystal obtained by filtration (ca. yield 5.652 g, 0.670 mmol, 18.3 % based on W). IR (KBr): $\bar{\upsilon}$ = 1597.8 (m), 1162.9 (s), 1076.4 (s), 1019.2 (w), 912.1 (m), 785.9 (m) cm^{-1}. ^{31}P NMR (D_2O): δ = -9.34 ppm. Negative ion MS (H_2O-CH_3OH): calcd. For $H_7K[P_5W_{30}O_{110}Na(H_2O)]^{6-}$ 1252.9775; found 1252.9747.

Preparation of $K_{12.5}Na_{1.5}[P_5W_{28.6}Mo_{1.4}O_{110}Na(H_2O)]-33H_2O$ (W:Mo = 27:3), $K_{12}Na_2[P_5W_{27.9}Mo_{2.1}O_{110}Na(H_2O)]-44H_2O$ (W:Mo = 25:5), $K_{12.5}Na_{1.5}[P_5W_{27.4}Mo_{2.6}O_{110}Na(H_2O)]-37H_2O$ (W:Mo = 22:8) and $K_{12.5}Na_{1.5}[P_5W_{26.5}Mo_{3.5}O_{110}Na(H_2O)]-45H_2O$ (W:Mo = 20:10) Na_2WO_4-2H_2O and Na_2MoO_4-2H_2O (29.380 g (89.1 mmol) and 2.060 g (8.5 mmol) for W:Mo = 27:3, 26.440 g (80.0 mmol) and 4.120 g (16.9 mmol) for W:Mo = 25:5, 23.510 g (71.2 mmol) and 6.180 g (25.5 mmol) for W:Mo = 22:8, and 20.570 g (62.9 mmol) and 8.240 g (33.9 mol) for W:Mo = 20:10, respectively,) were mixed with water (30 mL) in a Teflon-lined autoclave reactor, and phosphoric acid (85%, 26.5 mL) was added to the mixture. The reactor was placed in an oven heated at 125 °C for 24 h, and then the reactor was cooled down to room temperature. The yellowish green crystal was obtained which was filtered from the reaction mixture. The water (20 mL) was added to the filtrate followed by addition KCl (10.0 g), and the mixture was stirred for 10 min. The formed precipitates were filtered off, and the solid was dried at 70 °C overnight to obtain whitish green crude solid (ca. 4.02 g for W:Mo = 27:3, ca. 7.06 g for W:Mo = 25:5, ca. 9.6 g for W:Mo = 22:8, and ca. 9.88 g for W:Mo = 20:10, respectively). The solid were recrystallized from hot water (95 ºC, 10 mL for W:Mo = 27:3, 15 mL for W:Mo = 25:5, 17 mL for W:Mo = 22:8, and 17 mL for W:Mo = 20:10, respectively,) using a metal bath and obtained the whitish green crystal which were collected by filtration (yield ca. 2.182 g for W:Mo = 27:3, ca. 4.14 g for W:Mo = 25:5, ca. 5.30 g for W:Mo = 22:8, and ca. 5.12 g for W:Mo = 20:10, respectively). The solid were recrystallized again from hot water (95 ºC, 5 mL for W:Mo = 27:3, 7 mL for W:Mo = 25:5, 10 mL for W:Mo = 22:8, and 10 mL for W:Mo = 20:10, respectively) and the pure whitish green crystal obtained by filtration.

$K_{12.5}Na_{1.5}[P_5W_{28.6}Mo_{1.4}O_{110}Na(H_2O)]-33H_2O$ (yield 1.075 g, 0.127 mmol, 3.6 % based on W): IR (KBr): $\bar{\upsilon}$ = 1618.5 (m), 1164.7 (s), 1079.0 (s), 1017.4 (w), 910.2 (m), 796.9 (m) cm^{-1}. ^{31}P NMR (D_2O): δ = -8.47, -9.34, -9.49, and -9.70 ppm. Negative ion MS (H_2O-CH_3OH): calcd. For $H_7K[P_5W_{29}MoO_{110}Na(H_2O)]^{6-}$ 1238.1367; found 1238.1355. Elemental analysis: calculated: H 0.88, P 1.83, W 62.11, Mo 1.59, Na 0.68, K 5.77%; found H 0.69, P 1.81, W 62.07, Mo 1.34, Na 0.41, K 5.70%.

$K_{12}Na_2[P_5W_{27.9}Mo_{2.1}O_{110}Na(H_2O)]$ -44H_2O (yield 2.156 g, 0.251 mmol, 7.8 % based on W). IR (KBr): $\bar{\upsilon}$ = 1616.7 (m), 1161.9 (s), 1088.1 (s), 1019.4 (w), 934.6 (m), 782.1 (m) cm^{-1}. ^{31}P NMR (D_2O): δ = -8.47, -9.34, -9.49, and -9.70 ppm. Negative ion MS (H_2O-CH_3OH): calcd. For $H_7K[P_5W_{29}MoO_{110}Na(H_2O)]^{6-}$ 1238.1367; found 1238.1359. Elemental analysis: calculated: H 1.12, P 1.80, W 59.68, Mo 2.34, Na 0.80, K 5.46%; found H 0.76, P 1.75, W 59.44, Mo 2.04, Na 0.54, K 5.50%.

$K_{12.5}Na_{1.5}[P_5W_{27.4}Mo_{2.6}O_{110}Na(H_2O)]-37H_2O$ (yield 2.123 g, 0.252 mmol, 8.62 % based on W). IR (KBr): $\bar{\upsilon}$ = 1619.6 (m), 1163.7 (s), 1079.5 (s), 1016.5 (w), 913.9 (m), 784.1 (m) cm^{-1}. ^{31}P NMR (D_2O): δ = -8.47, -9.34, -9.49, and -9.70 ppm. Negative ion MS (H_2O-CH_3OH): calcd. For $H_7K[P_5W_{29}MoO_{110}Na(H_2O)]^{6-}$ 1238.1367; found 1238.1337. Elemental analysis: calculated: H 0.98, P 1.84, W 59.74, Mo 2.96, Na 0.68, K 5.80%; found H 0.63, P 1.77, W 59.93, Mo 2.72, Na 0.41, K 5.93%.

$K_{12.5}Na_{1.5}[P_5W_{26.5}Mo_{3.5}O_{110}Na(H_2O)]-45H_2O$ (yield 2.123 g, 0.250 mmol, 9.46 % based on W). IR (KBr): $\bar{\upsilon}$ = 1615.5 (m), 1163.9 (s), 1079.2 (s), 1016.4 (w), 932.6 (m), 786.6 (m) cm^{-1}. ^{31}P NMR (D_2O): δ = -8.47, -9.34, -9.49, and -9.70 ppm. Negative ion MS (H_2O-CH_3OH): calcd. For $H_7K[P_5W_{29}MoO_{110}Na(H_2O)]^{6-}$ 1238.1367; found 1238.1334. Elemental analysis: calculated: H 1.16, P 1.82, W 57.33, Mo 3.95, Na 0.68, K 5.75%; found H 0.78, P 1.76, W 57.12, Mo 3.95, Na 0.42, K 5.80%.

Other analytical techniques. Infrared (IR) spectra were recorded on a NICOLET 6700 FT-IR spectrometer (Thermo Fisher Scientific) as KBr pellets. ^{31}P NMR spectra were recorded on a Varian system 500 (500 MHz) spectrometer (Agilent) (P resonance frequency: 202.333 MHz). The spectra were referenced to external 85% H_3PO_4 (0 ppm). Cyclic voltammetry (CV) was performed on a CHI620D system (BAS Inc.) at ambient temperature. A glassy carbon working electrode (diameter, 3 mm), a platinum wire counter electrode, and an Ag/AgCl reference electrode (203 mV vs NHE at 25 °C) (3 M NaCl, BAS Inc.) were used. Elemental analyses were carried out by Analysis Center at Mitsubishi Chemical Co. (Ootake, Japan). High-resolution ESI-MS spectra were recorded on an LTQ Orbitrap XL (Thermo Fisher Scientific) with an accuracy of 3 ppm. Each sample (5 mg) was dissolved in 5 ml of H_2O, and the solutions were diluted by CH_3OH (final concentration: ca. 10 μg/ml). All peak assignment were done with accuracy less than 3 ppm.

Electronic Structure Calculations

Density functional theory (DFT) calculations were carried out on several isomers of the title structure with the ADF 2016 suite of programs.[49,50] Equilibrium geometries were obtained upon full geometry optimizations with tight convergence criteria[51] and the OPBE functional[52,53] with triple-ζ + double polarization atomic basis sets. The time-saving frozen core approximation was applied for the following atomic shells: 1s-2p for Na, 1s-2p for P, 1s-3d for Mo, 1s-4f for W and 1s for O. We simulated an aqueous solution (dielectric constant, ε = 78.4) by including the effects of solvent and counterions by means of the *conductor-like screening model* (COSMO).[54-57]

Single crystal X-ray diffraction analysis

Single crystals suitable for X-ray diffraction produced by recrystallization of $K_{12.5}Na_{1.5}[P_5W_{26.5}Mo_{3.5}O_{110}Na(H_2O)]$ from hot water were selected using

a microscope and mounted on a goniometer head using a LithoLoop. Intensity data were collected at 100 K on a Rigaku 1/4χ goniometer with a PILATUS3 X CdTe 1 M detector using synchrotron radiation (λ=0.4126 Å) monochromated by a Si (311) double crystal at SPring-8 (BL02B1 beamline). Data reduction was performed using RAPID AUTO. Absorption correction was performed by multi-scan method implemented in ABSCOR. The structures were solved by direct methods using SHELXS-2014.[62] The structure refinements were carried out using fullmatrix least-squares (SHELXL-2018/3).[62] All nonhydrogen atoms were refined anisotropically. Hydrogen atoms on water molecules were not located. Global ISOR restraints were applied for O and P atoms. Each metal centres at M_n (n = 6-15) was refined as two positionally disordered metal ions (W_n/Mo_n) with free variable site occupancies, x and 1-x. EADP and EXYZ constraints were applied for these disordered two metal centres to fix atomic displacement parameters and coordinates, respectively. Twelve diffractions were omitted to improve the data quality. Crystallographic data were summarized in Table S2, and further details of the crystal structure investigation can be obtained from Fachinformationszentrum Karlsruhe, 76344 Eggenstein-Leopoldshafen, Germany (fax: +49-7247-808-666; e-mail: crysdata@fiz-karlsruhe.de; http://www.fiz-karlsruhe.de/request_for_deposited_data.html on quoting the deposition number CSD-XXXXXXX.

Acknowledgements

This research was supported by JSPS KAKENHI Grant Number JP21H02028 and JP18H02058 (Grant-in-aid for scientific research (B)), Grant-in-Aid for Transformative Research Area (A) “Supra-ceramics” (JSPS KAKENHI Grant Number JS22H05144), International Network on Polyoxometalate Science at Hiroshima University, JSPS Core-to-Core program, and Takahashi Industrial and Economic Research Foundation (12-003-147). MNKW gratefully acknowledges the financial support from the Indonesia Endowment Fund for Education (LPDP), Ministry of Finance, Republik Indonesia for PhD scholarship (PRJ-36/ LPDP.3/2017). XL thanks the financial support of the Spanish Government (grant nr. PID2020-112762GB-I00). We thank Ms. T. Amimoto at the Natural Science Center for Basic Research and Development (N-BARD), Hiroshima University, for the ESI-MS measurements. We thank Mitsubishi Chemical Co. for ICP measurement. The synchrotron radiation experiment was performed on BL02B1 at Spring-8 with the approval of the Japan Synchrotron Radiation Research Institute (JASRI) (Proposal No. 2020 A1795).

Keywords: Polyoxometalate • Preyssler-type phosphotungstate • Substitution • Molybdate • Assembly

[1] M. T. Pope, *Heteropoly and Isopoly Oxometalates*, Springer-Verlag Berlin, **1983**, pp 1-196.

[2] (a) C. L. Hill, Thematic issue on Polyoxometalates, *Chem. Rev.*, **1998**, *98*, 327–358; (b) L. Cronin and A. Müller, Thematic issue on Polyoxometalates, *Chem. Soc. Rev*, **2012**, *41*, 7333−7334.

[3] M. Sadakane, Y. Ichi, Y. Ide and T. Sano, *Z. Anorg. Allg. Chem.*, **2011**, *637*, 2120–2124.

[4] K. Takahashi, T. Sano and M. Sadakane, *Z. Anorg. Allg. Chem.*, **2014**, *640*, 1314–1321.

[5] A. Hayashi, H. Ota, X. López, N. Hiyoshi, N. Tsunoji, T. Sano and M. Sadakane, *Inorg. Chem.,* **2016**, *55*, 11583-11592.

[6] A. Hayashi, M. N. K. Wihadi, H. Ota, X. López, K. Ichihashi, S. Nishihara, K. Inoue, N. Tsunoji, T. Sano and M. Sadakane, *ACS Omega*, **2018**, *3*, 2363–2373.

[7] F. F. Bamoharram, M. M. Heravi, M. Roshani, M. Jahangir and A. Gharib, *J. Mol. Catal. A-Chem.,* **2007**, *271*, 126–130.

[8] F. F. Bamoharram, M. M. Heravi, M. Roshani, M. Jahangir and A. Gharib, *Appl. Catal. A- Gen.*, **2006**, *302*, 42-47.

[9] M. M. Heravi, F. K. Behbahani and F. F. Bamoharram, *J. Mol. Catal. A. Chem.*, **2006**, *253*, 16–19.

[10] M. M. Heravi, K. Bakhtiari, Z. Daroogheha and F. F. Bamoharram, *Catal. Commun.*, **2007**, *8*, 1991-1994.

[11] R. Hekmatshoar, M. M. Heravi, S. Sadjadi, H. A. Oskooie and F. F. Bamoharram, *Catal. Commun.*, **2008**, *9*, 837-841.

[12] N. Feizi, H. Hassani and M. Hakimi, *Bull. Korean Chem. Soc.*, **2005**, *26*, 2087.

[13] C. Kato, R. Machida, R. Maruyama, R. Tsunashima, X.-M. Ren, M. Kurmoo, K. Inoue and S. Nishihara, *Angew. Chem. Int. Ed.,* **2018**, *57*, 13429-13432.

[14] S. Cardona-Serra, J. M. Clemente-Juan, E. Coronado, A. Gaita-Ariño, A. Camón, M. Evangelisti, F. Luis, M. J. Martínez-Pérez and J. Sesé, *J. Am. Chem. Soc.,* **2012**, *134*, 14982–14990.

[15] M. Zhu, T. Iwano, M. Tan, D. Akutsu, S. Uchida, G. Chen and X. Fang, *Angew. Chem. Int. Ed.*, **2022**, *61*, e202200666.

[16] T. Iwano, K. Shitamatsu, N. Ogiwara, M. Okuno, Y. Kikukawa, S. Ikemoto, S. Shirai, S. Muratsugu, P. G. Waddell, R. J. Errington, M. Sadakane and S. Uchida, *ACS Appl. Mater. Interfaces*, **2021**, *13*, 19138–19147.

[17] A. Amini, M. Rahimi, M. Nazari, C. Cheng and B. Samali, *RSC Advances*, **2019**, *9*, 2772–2783.

[18] T. Iwano, S. Miyazawa and S. Uchida, *Inorg. Chim. Acta*, **2020**, *499*, 119204.

[19] T. Iwano, S. Miyazawa, R. Osuga, J. N. Kondo, K. Honjo, T. Kitao, T. Uemura and S. Uchida, *Commun. Chem.,* **2019**, *2*, 9.

[20] S. Sun, L.-J. Zhu, K. Li, D.-M. Cheng, B. Li, Y.-H. Wang, H.-Y. Zang and Y.-G. Li, *Polyhedron*, **2019**, *169*, 84–88.

[21] K. Niinomi, S. Miyazawa, M. Hibino, N. Mizuno and S. Uchida, *Inorg. Chem.*, **2017**, *56*, 15187-15193.

[22] L. Chen, K. A. San, M. J. Turo, M. Gembicky, S. Fereidouni, M. Kalaj and A. M. Schimpf, *J. Am. Chem. Soc.*, **2019**, *141*, 20261-20268.

[23] N. Ogiwara, T. Iwano, T. Ito and S. Uchida, *Coord. Chem. Rev.*, **2022**, *462*, 214524.

[24] K. Sahiro, Y. Kawato, K. Koike, T. Sano, T. Nakai and M. Sadakane, *Sci. Rep.,* **2022**, *12*, 7554.

[25] S. F. Razavi, F. F. Bamoharram, T. Hashemi, K. Shahrokhabadi and A. Davoodnia, *Toxicol in Vitro*, **2020**, *68*, 104917.

[26] D. Kobayashi, Y. Ouchi, M. Sadakane, K. Unoura and H. Nabika, *Chem. Lett.*, **2017**, *46*, 533–535.

[27] N. I. Gumerova, E. Al-Sayed, L. Krivosudský, H. Čipčić-Paljetak, D. Verbanac and A. Rompel, *Front. Chem.*, **2018**, *6*, 336.

[28] K. Chen, Q. Yu, Y. Liu and P. Yin, *J. Inorg. Biochem.*, **2021**, *220*, 111463.

[29] A. Haider, K. Zarschler, S. A. Joshi, R. M. Smith, Z. Lin, A. S. Mougharbel, U. Herzog, C. E. Müller, H. Stephan and U. Kortz, *Z. Anorg. Allg. Chem.*, **2018**, *644*, 752–758.

[30] B. Fan, N. Cui, Z. Xu, K. Chen, P. Yin, K. Yue and W. Tang, *Biomacromolecules*, **2022**, *23*, 972–982.

[31] M. H. Alizadeh, S. P. Harmalker, Y. Jeannin, J. Martin-Frere and M. T. Pope, *J. Am. Chem. Soc.* **1985**, *107*, 2662-2669.

[32] M. N. K. Wihadi, A. Hayashi, T. Ozeki, K. Ichihashi, H. Ota, M. Fujibayashi, S. Nishihara, K. Inoue, N. Tsunoji, T. Sano and M. Sadakane, *Bull. Chem. Soc. Jpn.*, **2020**, *93*, 461-466.

[33] I. Creaser, M. C. Heckel, R. J. Neitz and M. T. Pope, *Inorg. Chem.*, **1993**, *32*, 1573-1578.

[34] M. H. Dickman, G. J. Gama, K.-C. Kim and M. T. Pope, *J. Cluster Sci.,* **1996**, *7*, 567–583.

[35] C. W. Williams, M. R. Antonio and L. Soderholm, *J. Alloys Compd.,* **2000**, *303–304*, 509–513.
[36] K. Shitamatsu, T. Kojima, P. G. Waddell, Sugiarto, H. E. Ooyama, R. J. Errington, M. Sadakane, *Z. Anorg. Allg. Chem.*, **2021**, *647*, 1239–1244
[37] K. C. Kim, M. T. Pope, G. J. Gama and M. H. Dickman, *J. Am. Chem. Soc.,* **1999**,*121*, 11164-11170.
[38] M. R. Antonio and M. H. Chiang, *Inorg. Chem.,* **2008**, *47*, 8278-8285.
[39] A. Hayashi, T. Haioka, K. Takahashi, B. S. Bassil, U. Kortz, T. Sano and M. Sadakane, *Z. Anorg. Allg. Chem.*, **2015**, *641*, 2670–2676.
[40] J. Du, M.-D. Cao, S.-L. Feng, F. Su, X.-J. Sang, L.-C. Zhang, W.-S. You, M. Yang and Z.-M. Zhu, *Chem. Eur. J.*, **2017**, *23*, 14614–14622.
[41] M.-X. Liang, C.-Z. Ruan, D. Sun, X.-J. Kong, Y.-P. Ren, L.-S. Long, R.-B. Huang and L.-S. Zheng, *Inorg. Chem.*, **2014**, *53*, 897-902.
[42] C. Kato, K. Y. Maryunina, K. Inoue, S. Yamaguchi, H. Miyaoka, A. Hayashi, M. Sadakane, R. Tsunashima and S. Nishihara, *Chem. Lett.*, **2017**, *46*, 602–604.
[43] A.-X. Tian, Y. Yang, H.-P. Ni, G.-Y. Liu, Y.-B. Fu, M.-L. Yang, G.-C. Liu and J. Ying, *Transit. Met. Chem.,* **2018**, *44*, 303-309.
[44] T.-P. Hu, Y.-Q. Zhao, Z. Jaglič, K. Yu, X.-P. Wang and D. Sun, *Inorg. Chem*, **2015**, *54*, 7415–7423.
[45] M. N. K. Wihadi and M. Sadakane, *Z. Anorg. Allg. Chem.*, **2020**, *646*, 1297-1302.
[46] M. Arabi, M. M. Amini, M. Abedini, A. Nemati and M. Alizadeh, *J. Mol. Catal. A-Chem.,* **2003**, *200*, 105–110.
[47] D. M. Ruiz, G. P. Romanelli, P. G. Vázquez and J. C. Autino, *Appl. Catal. A- Gen.,* **2010**, *374*, 110–119.
[48] G. Romanelli, D. Ruiz, P. Vázquez, H. Thomas and J. C. Autino, *Chem. Eng. J.,* **2010**, *161*, 355-362.
[49] C. Fonseca Guerra, J. G. Snijders, G. Te Velde, E. J. Baerends, *Theor. Chem. Acc.* **1998,** *99*, 391-403.
[50] G. te Velde, F. M. Bickelhaupt, E. J. Baerends, C. Fonseca Guerra, S. J. A. van Gisbergen, J. G. Snijders, T. Ziegler, *J. Comput. Chem.* **2001,** *22*, 913-967.
[51] Optimized structures must be very accurate when frequency calculations are to be conducted since molecular vibrations can be highly dependent on geometrical parameters.
[52] N. C. Handy, A. J. Cohen, *Mol. Phys.* **2001,** *99*, 403-412.
[53] M. Swart, A. W. Ehlers, K. Lammertsma, *Mol. Phys.* **2004,** *102*, 2467-2474.
[54] A. Klamt, G. Schüürmann, *J. Chem. Soc., Perkin Trans.* **1993,** *2*, 799-805.
[55] J. Andzelm, C. Kölmel, A. Klamt, *J. Chem. Phys.* **1995,** *103*, 9312
[56] A. Klamt, *J. Phys. Chem.* **1995,** *99*, 2224-35.
[57] C. C. Pye, T. Ziegler, *Theor. Chem. Acc.* **1999,** *101*, 396-408.
[58] M. Abbessi, R. Contant, R. Thouvenot and G. Herve, *Inorg. Chem.*, **1991**, *30*, 1695–1702.
[59] U. B. Mioč, M. R. Todorović, M. Davidović, P. Colomban and I. Holclajtner-Antunović, *Solid State Ion.*, **2005**, *176*, 3005–3017.
[60] M.-H. Chiang, M. R. Antonio, C. W. Williams and L. Soderholm, *Dalton Trans.*, **2004**, *5*, 801-806.
[61] T. Ueda, T. Toya, M. Hojo, *Inorg. Chim. Acta*, **2004**, *357*, 59-65.
[62] G. M. Sheldrick, *Acta Cryst.*, **2008**, *A64*, 112–113.

Entry for the Table of Contents

Layout 2:

FULL PAPER

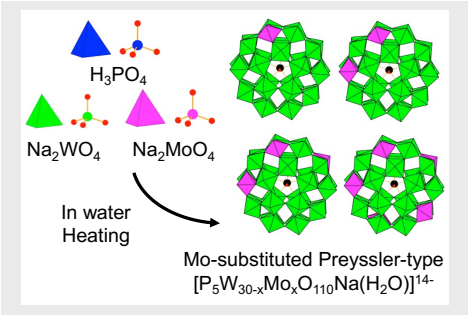

Reaction of Na_2WO_4 and Na_2MoO_4 in the presence of H_3PO_4 produces multi-Mo-substituted Preyssler-type phosphotungstate, $[P_5W_{30-x}Mo_xO_{110}Na(H_2O)]^{14-}$ (x up to 5).

Key Topic*

*M. N. K. Wihadi, T. Haioka, T. Kojima, X. López, T. Ueda, T. Sano, M. Sadakane**

Page No. – Page No.

Synthesis and Structural Characterization of Multi-Molybdenum substituted Preyssler-type Phosphotungstates